# Letters to *Analytical Chemistry*

# Pyrene-Functionalized Ruthenium Nanoparticles as Effective Chemosensors for Nitroaromatic Derivatives

**Wei Chen, Nathaniel B. Zuckerman, Joseph P. Konopelski, and Shaowei Chen***

*Department of Chemistry and Biochemistry, University of California, 1156 High Street, Santa Cruz, California 95064*

**Pyrene-functionalized Ru nanoparticles were synthesized by olefin metathesis reactions of carbene-stabilized Ru nanoparticles with 1-vinylpyrene and 1-allylpyrene (the resulting particles were denoted as Ru=VPy and Ru=APy, respectively) and examined as sensitive chemosensors for the detection of nitroaromatic compounds, such as 2,4,6-trinitrotoluene (TNT), 2,4-dinitrotoluene (2,4-DNT), 2,6-dinitrotoluene (2,6-DNT), 1-chloro-nitrobenzene (CNB), and nitrobenzene (NB), by their effective quenching of the nanoparticle fluorescence. It was found that the detection sensitivity increased with increasing nitration of the molecules. Additionally, in comparison to monomeric pyrene derivatives, both Ru=VPy and Ru=APy nanoparticles exhibited markedly enhanced performance in the detection of nitroaromatic explosives, most probably as a result of the enhanced collision frequency between the fluorophores and the quencher molecules. Furthermore, Ru=VPy nanoparticles displayed much higher sensitivity (down to the nanomolar regime for TNT) than Ru=APy in the detection of these nitroaromatic explosives, which was ascribed to the extended intraparticle conjugation that provided efficient pathways for energy/electron transfer and consequently amplified the analyte binding events.**

Chemical sensors with high sensitivity and selectivity for the detection of nitroaromatics, especially 2,4,6-trinitrotoluene (TNT), have attracted much attention from the military and homeland security points of view, because of the wide applications of these compounds as explosive materials.[1] Various analytical methods have been developed for the sensitive detection of nitroaromatic compounds that are based on, for instance, chromatography,[2] amperometry,[3] surface-enhanced Raman spectroscopy,[4] energy-dispersive X-ray analysis,[5] etc. In recent years, photoluminescence-based chemosensors that exploit sensitive fluorescence quenching by nitroaromatic derivatives have also been investigated rather extensively.[6–12] In comparison with other methods, fluorescence-based detection has the notable advantages of high sensitivity and detection simplicity for both vapor and solution phases of nitroaromatic explosives at low concentrations. For instance, conjugated polymers have been shown to provide efficient detection for the electron-deficient nitroaromatic compounds,[8,13–16] which is attributed to the amplified response to the analyte binding event. This amplification effect is usually considered to arise from the efficient transfer of excitation energy from large areas in the conjugated polymers to the sites of analyte binding.[13] Yet the synthesis of these functional polymers is nontrivial, and the detection analysis may be complicated by the dispersity of the polymer size and structures. In other studies, semiconductor quantum dots and nanocrystals modified with different surface functional groups have also been examined as fluorescence sensors for the detection of nitroaromatic compounds by taking advantage of their unique photoluminescence characteristics.[17] However, it should be noted that quantum dots that are made of compound semiconductors are generally prone to photodegradation that might compromise their stability and durability.

In this letter, we carry out a study to examine the application of pyrene-functionalized ruthenium nanoparticles as effective

---

* To whom correspondence should be addressed. E-mail: schen@chemistry.ucsc.edu.

(1) Fainberg, A. *Science* **1992**, *255*, 1531–1537.
(2) Weisberg, C. A.; Ellickson, M. L. *Am. Lab.* **1998**, *30*, 32N–+.
(3) Hilmi, A.; Luong, J. H. T. *Anal. Chem.* **2000**, *72*, 4677–4682.
(4) Sylvia, J. M.; Janni, J. A.; Klein, J. D.; Spencer, K. M. *Anal. Chem.* **2000**, *72*, 5834–5840.
(5) Luggar, R. D.; Farquharson, M. J.; Horrocks, J. A.; Lacey, R. J. *X-Ray Spectrom.* **1998**, *27*, 87–94.

(6) Grose, J. E.; Pasupathy, A. N.; Ralph, D. C.; Ulgut, B.; Abruna, H. D. *Phys. Rev. B* **2005**, *71*, 035306.
(7) Naddo, T.; Che, Y. K.; Zhang, W.; Balakrishnan, K.; Yang, X. M.; Yen, M.; Zhao, J. C.; Moore, J. S.; Zang, L. *J. Am. Chem. Soc.* **2007**, *129*, 6978.
(8) Mcquade, D. T.; Pullen, A. E.; Swager, T. M. *Chem. Rev.* **2000**, *100*, 2537–2574.
(9) Toal, S. J.; Magde, D.; Trogler, W. C. *Chem. Commun.* **2005**, 5465–5467.
(10) Sohn, H.; Sailor, M. J.; Magde, D.; Trogler, W. C. *J. Am. Chem. Soc.* **2003**, *125*, 3821–3830.
(11) Sohn, H.; Calhoun, R. M.; Sailor, M. J.; Trogler, W. C. *Angew. Chem., Int. Ed.* **2001**, *40*, 2104–2105.
(12) Content, S.; Kirschdemesmaeker, A. *J. Chem. Soc., Faraday Trans.* **1997**, *93*, 1089–1094.
(13) Yang, Y. F.; Zhou, Y. H.; Cha, C. S. *Electrochim. Acta* **1995**, *40*, 2579–2586.
(14) Li, J.; Kendig, C. E.; Nesterov, E. E. *J. Am. Chem. Soc.* **2007**, *129*, 15911–15918.
(15) Yang, J. S.; Swager, T. M. *J. Am. Chem. Soc.* **1998**, *120*, 11864–11873.
(16) Narayanan, A.; Varnavski, O. P.; Swager, T. M.; Goodson, T. *J. Phys. Chem. C* **2008**, *112*, 881–884.
(17) Tu, R. Y.; Liu, B. H.; Wang, Z. Y.; Gao, D. M.; Wang, F.; Fang, Q. L.; Zhang, Z. P. *Anal. Chem.* **2008**, *80*, 3458–3465.

---

chemosensors for the detection of nitroaromatic derivatives, which exhibited marked enhancement of the detection sensitivity and selectivity as compared to monomeric pyrene and derivatives.[18−20] One may note that the application of functional metal nanoparticles as effective chemosensors for explosive detection has actually been relatively scarce, despite their clear advantages of simple synthetic procedures and robust structures.

Experimentally, the pyrene moieties were bound onto the Ru nanoparticle surface through olefin metathesis reactions by conjugated Ru=carbene $\pi$ bonds.[21] Because of these conjugated interfacial metal−ligand bonding interactions, extended intraparticle conjugation might occur depending on the chemical linkers that bound the pyrene moieties onto the particle surface. That is, the nanoparticle metallic core served as a conducting medium for intraparticle charge delocalization, leading to the appearance of novel photoluminescence characteristics that resembled those of pyrene dimers with a conjugated spacer.[21−23] Consequently, these pyrene-functionalized nanoparticles behaved analogously to pyrene conjugated polymers in the binding and detection of nitroaromatic compounds. Within this context, we examine in detail the quenching effects of five nitroaromatic compounds, 2,4,6-trinitrotoluene (TNT), 2,4-dinitrotoluene (2,4-DNT), 2,6-dinitrotoluene (2,6-DNT), nitrobenzene (NB), and 1-chloro-nitrobenzene (CNB) on the fluorescence of Ru nanoparticles that underwent metathesis reactions with 1-vinylpyrene or 1-allylpyrene (the resulting particles were denoted as Ru=VPy and Ru=APy, respectively). The results show that overall both nanoparticles exhibited marked enhancement in the detection of these nitroaromatic derivatives, as compared to monomeric pyrene, and more importantly, Ru=VPy particles offered a significantly greater sensitivity (down to the nanomolar regime for TNT, for instance) than the Ru=APy counterparts.

## EXPERIMENTAL SECTION

**Materials.** 2,4,6-Trinitrotoluene (TNT, 99.5%, Chem Service), 2,4-dinitrotoluene (2,4-DNT, 99.3%, Ultra Scientific), 2,6-dinitrotoluene (2,6-DNT, 99.74%, Ultra Scientific), nitrobenzene (NB, Mallinckrodt), and 1-chloro-nitrobenzene (CNB, 99.5%, Chem Service), ruthenium chloride (RuCl$_3$, 99+%, ACROS), 1,2-propanediol (ACROS), sodium acetate trihydrate (NaAc·3H$_2$O, MC&B), and extra dry *N,N*-dimethylformamide (DMF, 99.8%, Aldrich) were all used as received. Solvents were obtained from typical commercial sources and were used without further treatment. Water was supplied by a Barnstead Nanopure water system (18.3 MΩ cm).

The preparation and characterization of pyrene-functionalized ruthenium nanoparticles, i.e., Ru=VPy and Ru=APy, have been described in detail previously.[21] Briefly, carbene-stabilized Ru nanoparticles were first prepared by mixing octyl diazoacetate with ruthenium colloids that were formed by thermolysis of RuCl$_3$ in 1,2-propanediol because of the strong affinity of the diazo functional group to Ru surfaces. The nanoparticles exhibited a core diameter of 2.12 ± 0.72 nm as determined by transmission electron microscopy (TEM) measurements.[24] After metathesis reactions with pyrene derivatives, the Ru nanoparticles were subject to extensive rinsing to remove free organic ligands, and the surface concentration of the pyrene moieties was estimated by $^1$H NMR measurements to be 26.4% and 22.9% for the Ru=VPy and Ru=APy nanoparticles, respectively.[21] With a nanoparticle composition of Ru$_{367}$L$_{71}$ (with L being the surface ligands),[23] this indicates that there were approximately 19 and 16 pyrene moieties on these two nanoparticles.

**Fluorescence Spectroscopy.** Fluorescence measurements were carried out with a PTI fluorospectrometer. In a typical procedure, 2 mL of a Ru=VPy nanoparticle solution at a concentration of 0.05 mg/mL in DMF was added to a quartz cuvette. A calculated amount of a nitroaromatic analyte was then injected into the cuvette. Fluorescence spectra were collected after thorough mixing of the analyte with the nanoparticle solution. The same procedure was used in the quenching measurements with Ru=APy nanoparticles and simple pyrene derivatives.

## RESULTS AND DISCUSSION

Figure 1A shows a series of fluorescence emission spectra of Ru=VP nanoparticles in DMF (0.05 mg/mL) with the addition of varied amounts of TNT (within the range of 20 nM to 30 $\mu$M, shown as figure legends). As shown previously,[21] Ru=VPy nanoparticles exhibited two prominent emission peaks at 392 and 490 nm, with the former consistent with that of monomeric pyrene moieties and the latter arising from the extended intraparticle conjugation because of the Ru=C $\pi$ bonds. Interestingly, upon the introduction of TNT, the 392 nm emission peak exhibited a drastic diminishment whereas the 490 nm emission remained virtually invariant. Similar quenching behaviors of the Ru=VPy nanoparticle fluorescence were also observed with other nitroaromatic compounds such as 2,4-DNT, 2,6-DNT, NB, and CNB (Supporting Information, Figure S1).

It has been known that fluorescence quenching mainly follows two mechanisms, static quenching and dynamic quenching.[25,26] The former entails the formation of a stable complex between a fluorophore and a quencher both at ground state; whereas the latter refers to the formation of a transient complex between an excited-state fluorophore and a ground-state quencher. Because the latter is a consequence of physical collision, the quenching efficiency is concentration-dependent, which is represented by the Stern−Volmer equation,
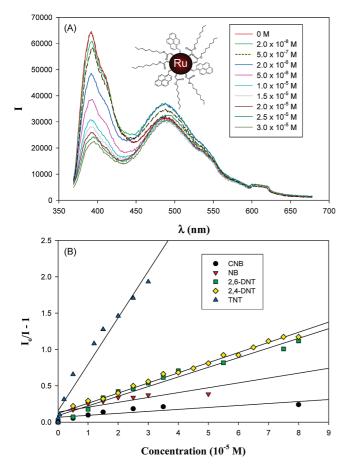
$$\frac{I_o}{I} - 1 = k\tau_o C_A = K_{SV} C_A \qquad (1)$$

where $I_o$ and $I$ are the fluorescence intensity in the absence and presence of analyte (quencher, A), respectively, $C_A$ is the molar concentration of the analyte, $k$ is the bimolecular rate

(18) Goodpaster, J. V.; McGuffin, V. L. *Anal. Chem.* **2001**, *73*, 2004–2011.
(19) Focsaneanu, K. S.; Scaiano, J. C. *Photochem. Photobiol. Sci.* **2005**, *4*, 817–821.
(20) Hughes, A. D.; Glenn, I. C.; Patrick, A. D.; Ellington, A.; Anslyn, E. V. *Chem.—Eur. J.* **2008**, *14*, 1822–1827.
(21) Chen, W.; Zuckerman, N. B.; Lewis, J. W.; Konopelski, J. P.; Chen, S. W. *J. Phys. Chem. C* **2009**, *113*, 16988–16995.
(22) Chen, W.; Brown, L. E.; Konopelski, J. P.; Chen, S. W. *Chem. Phys. Lett.* **2009**, *471*, 283–285.
(23) Chen, W.; Chen, S. W.; Ding, F. Z.; Wang, H. B.; Brown, L. E.; Konopelski, J. P. *J. Am. Chem. Soc.* **2008**, *130*, 12156–12162.
(24) Chen, W.; Davies, J. R.; Ghosh, D.; Tong, M. C.; Konopelski, J. P.; Chen, S. W. *Chem. Mater.* **2006**, *18*, 5253–5259.
(25) Lakowicz, J. R. *Principles of Fluorescence Spectroscopy*, 3rd ed.; Springer: New York, 2006.
(26) Badley, R. *Fluorescence Spectroscopy*; Plenum Press: New York, 1983.

**Figure 1.** (A) Fluorescence emission spectra of Ru=VPy nanoparticles (0.05 mg/mL in DMF; effective pyrene concentration 19 $\mu$M) with the addition of varied amounts of TNT (shown as figure legends). The excitation wavelength was set at 349 nm. The broad features between 530 and 650 nm were from solvent background. The inset shows a schematic of the nanoparticle structure. (B) Stern–Volmer plots of the Ru=VPy nanoparticles in the presence of different nitroaromatic analytes. The symbols are experimental data from panel A and Figure S1 in the Supporting Information, and the lines are the linear regression.

**Table 1. Quenching Constants ($K_{SV}$) of the Ru=VPy and Ru=APy Nanoparticles for Varied Nitroaromatic Compounds**

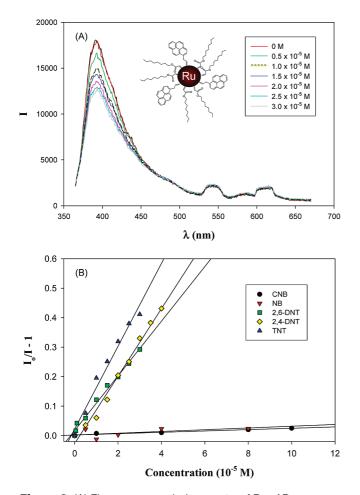| $K_{SV}$ (M$^{-1}$) | CNB | NB | 2,6-DNT | 2,4-DNT | TNT |
|---|---|---|---|---|---|
| Ru=VPy | $2.71 \times 10^3$ | $6.69 \times 10^3$ | $1.33 \times 10^4$ | $1.40 \times 10^4$ | $6.40 \times 10^4$ |
| Ru=APy | $2.28 \times 10^2$ | $2.96 \times 10^2$ | $9.27 \times 10^3$ | $1.14 \times 10^4$ | $1.40 \times 10^4$ |

M$^{-1}$, $1-5 \times 10^3$ M$^{-1}$, $3-5 \times 10^3$ M$^{-1}$, and $5.5 \times 10^3$ M$^{-1}$ by using chemosensors based on iptycene-units isolated polymers,[16] oligo(tetraphenyl)silole nanoparticles,[9] polymetalloles and polysilanes,[10,11] and amine-capped ZnS-Mn$^{2+}$ nanocrystals,[17] respectively. The significantly higher $K_{SV}$ values obtained in the present study suggest that the Ru=VPy nanoparticles might be exploited as effective chemosensors with enhanced sensitivity for the detection of nitroaromatic explosives.

Such high sensitivity toward nitroaromatic derivatives (in particular, TNT) may be accounted for by the effective charge transfer from the electron-rich pyrene to the electron-poor nitroaromatic compounds that can be readily manipulated by the number of nitro substituents. This may be understood within the context of the electronic energy structures of the pyrene moieties and nitroaromatic quenchers. Previously, using density functional theory calculations, Park and Cheong estimated the highest occupied molecular orbital (HOMO) and lowest unoccupied molecular orbital (LUMO) energy of pyrene to be about $-5.6$ and $-1.8$ eV, respectively;[27] whereas Yang and Swager reported that the reduction potentials ($E^o$ vs SCE) for nitroaromatic compounds exhibited an anodic shift with increasing nitration (and hence decreasing electron density): CNB, $-1.1$ V; NB, $-1.15$ V; 2,6-DNT, $-1.0$ V; 2,4-DNT, $-1.0$ V; and TNT, $-0.7$ V, respectively.[15] By taking advantage of the relationship between the formal potential ($E^o$ vs NHE) and the absolute electron potential ($E_{abs}$), $E_{abs} = -(E^o + 4.44)$ (electronvolts, at 298 K), the corresponding electronic energy was found at $-3.56$, $-3.51$, $-3.66$ eV, $-3.66$, and $-3.96$ eV, suggesting an energy landscape for the effective charge transfer of photogenerated electrons from the pyrene LUMO to the varied quencher molecules. In fact, according to the Rehm–Weller equation,[14] analytes with a less negative reduction potential are anticipated to exhibit a larger driving force for electron transfer from particles to quenchers. This is largely consistent with the experimental observation (Figure 1) where the quenching efficiency increases in the order of CNB < NB < 2,6-DNT $\approx$ 2,4-DNT < TNT.

Interestingly, the sensing performance exhibits a drastic variation with the chemical linker that binds the pyrene moieties onto the Ru particle surface. Ru=APy nanoparticles were used as the comparative example. Figure 2A shows the fluorescence profiles of Ru=APy nanoparticles with the addition of varied amounts of TNT (from 5 to 30 $\mu$M, shown as figure legends). It can be seen that Ru=APy exhibited a single well-defined emission peak at 394 nm, consistent with monomeric pyrene moieties, as demonstrated previously.[21] In contrast to Ru=VPy nanoparticles, the introduction of a sp$^3$ carbon into the chemical linkers effectively turned off the intraparticle charge delocalization and consequently the particle-bound pyrene moieties behaved individually. Upon the addition of TNT, the fluorescence

constant for the dynamic quenching, $\tau_o$ is the fluorescence lifetime of the unquenched fluorophore, and $K_{SV}$ ($= k\tau_o$) is the corresponding Stern–Volmer quenching constant.

On the basis of the quenching of the 392 nm emission of the Ru=VPy nanoparticles, Figure 1B depicts the Stern–Volmer plots in the presence of varied nitroaromatic compounds (CNB, NB, 2,6-DNT, 2,4-DNT, and TNT), from which at least two aspects warrant special attention. First, the linearity suggests that dynamic quenching plays the predominant role in the quenching of the Ru=VPy nanoparticle fluorescence. Second, the quenching constant varies rather significantly with the specific quencher, as manifested by the slopes of the Stern–Volmer plots, which are summarized in Table 1: CNB, $2.71 \times 10^3$ M$^{-1}$; NB, $6.69 \times 10^3$ M$^{-1}$; 2,6-DNT, $1.33 \times 10^4$ M$^{-1}$; 2,4-DNT, $1.40 \times 10^4$ M$^{-1}$; and TNT, $6.40 \times 10^4$ M$^{-1}$. It can be seen that the quenching constant for TNT is markedly larger than those for the other nitroaromatic compounds in the series. Importantly, these quenching constants are much higher than those with other luminescent chemosensors that are based on conjugated polymers or quantum dots reported in the literatures.[9–11,16,17] For instance, the quenching constants for TNT were found to be $0.73 \times 10^3$

(27) Park, Y. H.; Cheong, B. S. *Curr. Appl. Phys.* **2006**, *6*, 700–705.

**Figure 2.** (A) Fluorescence emission spectra of Ru=APy nanoparticles (0.05 mg/mL in DMF; effective pyrene concentration 16 $\mu$M) with the addition of varied amounts of TNT (shown as figure legends). Excitation wavelength was set at 349 nm. The broad features between 530 and 650 nm were from solvent background. The inset shows a schematic of the nanoparticle structure. (B) Stern−Volmer plots of the Ru=APy nanoparticles in the presence of different nitroaromatic analytes. The symbols are experimental data from panel A and Figure S2 in the Supporting Information, and the lines are the linear regression.

intensity showed an apparent decrease and similar behaviors were also observed with other nitroaromatic quenchers (Figure S2 in the Supporting Information), although the decay was not as dramatic as that observed with Ru=VPy nanoparticles (Figure 1).

Figure 2B shows the corresponding Stern−Volmer plots of the Ru=APy nanoparticles with the addition of varied amounts of CNB, NB, 2,6-DNT, 2,4-DNT, and TNT. Similar to Ru=VPy, the quenching followed the dynamic quenching mechanism, as manifested by the linear responses. From the slopes of the Stern−Volmer plots, the quenching constants were then estimated and listed in Table 1: CNB, $2.28 \times 10^2$ M$^{-1}$; NB, $2.96 \times 10^2$ M$^{-1}$; 2,6-DNT, $9.27 \times 10^3$ M$^{-1}$; 2,4-DNT, $1.14 \times 10^4$ M$^{-1}$; and TNT, $1.40 \times 10^4$ M$^{-1}$. From these, one may note that (i) the quenching becomes increasingly effective with increasing nitration of the quencher molecules, akin to the observation with Ru=VPy nanoparticles and (ii) the quenching constants are substantially smaller than those for the Ru=VPy nanoparticles (although the changing trend is similar).

It is most likely that the discrepancy observed above between the Ru=VPy and Ru=APy nanoparticles arose from the difference of the chemical linkers that bound the pyrene moieties onto the nanoparticle surface. In Ru=VPy nanoparticles (inset of Figure 1A), the conjugated Ru=C interfacial bonding interactions led to effective intraparticle charge delocalization and hence enhanced energy/electron transfer to the quencher molecules, analogous to the amplification effects observed previously with pyrene-based conjugated polymers.[14] However, such intraparticle extended conjugation was effectively turned off in Ru=APy (inset of Figure 2A) with the insertion of a sp$^3$ carbon into the chemical linker, thus decreasing the quenching efficiency.

It should be noted, however, that both nanoparticles exhibited far more drastic quenching by the nitroaromatic derivatives than pyrene monomers. For instance, the quenching constant of TNT for the fluorescence of 1-bromopyrene was merely $2.53 \times 10^3$ M$^{-1}$ (Figure S3 in the Supporting Information), more than 1 order of magnitude smaller than those for Ru=VPy and Ru=APy (Table 1). This may be ascribed to the close proximity of the pyrene moieties on the nanoparticle surface that most probably enhances the effective collision frequency with the quencher molecules, because the fluorescence lifetimes ($\tau_o$) of the series of fluorophores are very comparable (except for Ru=VPy which exhibits a lowest $\tau_o$ of 7 ns),[21] as dictated by the dynamic quenching mechanism (eq 1).

A further comparative study was carried out with (E)-1,2-di(pyren-1-yl)ethene. Previously we showed that because of the interfacial Ru=C $\pi$ bonds, Ru=VPy nanoparticles behaved equivalently to (E)-1,2-di(pyren-1-yl)ethene,[21] a pyrene dimer with a conjugated spacer (−CH=CH−), where both exhibited two emission peaks at 392 and 490 nm. Interestingly, they also showed similar quenching characteristics by nitroaromatic derivaties. For instance, even in the presence of up to 40 mM of nitroaromatic analytes, the emission features at 490 nm remained unchanged for (E)-1,2-di(pyren-1-yl)ethene (Figure S4 in the Supporting Information), consistent with that for Ru=VPy nanoparticles depicted in Figure 1. While the origin is not fully understood at this point, the results seem to suggest that the intraparticle conjugated structures most likely lower the LUMO energy such that charge transfer to the nitroaromatic quencher becomes impeded. Further studies are desired to address this issue.

Nevertheless, the consistent behaviors observed with (E)-1,2-di(pyren-1-yl)ethene further confirms that the 490 nm emission peak of the Ru=VPy nanoparticles is most likely due to intraparticle extended conjugation[21] and not to the formation of polymeric materials[23] or excimers.[28] Note that excimer emissions may be effectively quenched by nitroaromatics.[28] Additionally, as mentioned previously and shown here,[21] Ru=APy nanoparticles exhibited only a single emission peak, akin to pyrene monomers, despite similar surface structure and pyrene coverage to that on Ru=VPy (other experimental conditions were identical). Also, whereas the excitation spectra of Ru=APy and bromopyrene are very similar, an apparent red-shift can be seen in the excitation spectrum of Ru=VPy nanoparticles (Figure S5 in the Supporting Information). Note that if the emissions of Ru=VPy were indeed due to excimer formation, one would anticipate an excitation

(28) Burattini, S.; Colquhoun, H. M.; Greenland, B. W.; Hayes, W.; Wade, M. *Macromol. Rapid Commun.* **2009**, *30*, 459–463.

spectrum similar to that of monomeric pyrene.[29] No excimer emission was found either with gold nanoparticles covered with Py—CH$_2$NH$_2$.[30]

## CONCLUSIONS

In this study, pyrene-functionalized ruthenium nanoparticles were examined as potential chemosensors for the sensitive detection of nitroaromatic derivatives, key explosive components in a wide range of applications. The detection was based on the sensitive quenching of the fluorescence of the pyrene moieties in the presence of nitroaromatic compounds, as accounted for by the dynamic quenching mechanism. It was found that Ru=VPy nanoparticles exhibited much higher sensitivity than Ru=APy nanoparticles and pyrene monomers, in particular toward TNT with a detection limit down to nanomolar concentration. Further improvement of the detection performance is possible considering the fundamental insights gained from the study. First, enhanced quenching efficiency was observed when the fluorophores were immobilized on the nanoparticle surface as compared to the monomeric forms, most probably as a result of the enhanced collision frequency between the fluorophores and the quenchers. Second, extended intraparticle conjugation resulting from the interfacial metal—ligand $\pi$ bonds might enhance energy/charge transfer leading to amplified quenching of the fluorescence responses.

## SUPPORTING INFORMATION AVAILABLE

Additional fluorescence spectra of 1-bromopyrene, (E)-1,2-di(pyren-1-yl)ethene, Ru=VPy, and Ru=APy nanoparticles in the presence of varied nitroaromatic compounds. This material is available free of charge via the Internet at http://pubs.acs.org.

(29) Nakamura, M.; Saito, N.; Takayama, K.; Kumamoto, S.; Yamana, K. *Chem. Lett.* **2007**, *36*, 602–603.

(30) Thomas, K. G.; Kamat, P. V. *J. Am. Chem. Soc.* **2000**, *122*, 2655–2656.